Earthquake Engineering, Tenth World Conference © 1992 Balkema, Rotterdam. ISBN 90 5410 060 5

Seismic proving tests for nuclear power plant, no. 2

Yoshiaki Shimazaki
Mitsubishi Atomic Power Industries, Inc., Tokyo, Japan

Hiroshi Akiyama
University of Tokyo, Japan

Muneaki Kato
Japan Atomic Power Company, Tokyo, Japan

Shigeru Kusumoto
Nuclear Power Engineering Center, Tokyo, Japan

Katsuhisa Fujita, Eiji Yoshikawa & Koji Koyama
Mitsubishi Heavey Industries, Ltd, Tokyo, Japan

ABSTRACT: This paper presents a summary of the results of the PWR Seismic Proving Tests carried out in Japan. Four large test models (reactor containment vessel, reactor vessel, reactor core internals and primary coolant loop system) were vibrated on a shaking table to verify their strength and ability to function during earthquakes. Test results indicated that PWR key components have an adequate margin of safety and that the current seismic design analysis method is appopriate.

1. INTRODUCTION

Since 1982, a series of Proving Tests on the Seismic Reliability of nuclear power plants has been carried out by the Nuclear Power Engineering Center (NUPEC), using a Large-Scale High Performance Shaking Table Facility at Tadotsu Engineering Laboratory, under the sponsorship of the Ministry of International Trade and Industry (MITI) of Japan.

The first series of tests was carried out using test models [Containment Vessel (CV), Reactor Core Internals including Fuel Assemblies and Control Rods (CI), Reactor Vessel (RV), and Primary Coolant Loop System (RCS)] which were selected as key components in the equipment of Japanese standardized 1100 MWe nuclear power plants from the point of view of seismic reliability.

The main objectives of the PWR seismic proving tests are as follows.

(1) To confirm the integrity and strength of the equipment against earthquakes
(2) To confirm the functional intergity during and after earthquakes (for example, RCC insertion or leak tightness of the Containment Vessel)
(3) To confirm adequacy of the seismic design analysis method

In order to achieve these objectives, the test model, which is as similar as possible to the actual plant configuration, material, scale, etc. is tested under design earthquake conditions. The seismic safety and reliability of the models are directly confirmed by the test, and the adequacy of the design analysis method is also confirmed by the analysis of the test data.

2. TEST MODEL

The four key components (CV, RV, CI, RCS) were selected to be tested as they are the important ones from the standpoint of seismic safety.

Full scale or close to full scale models were chosen and they were manufactured by the same methods and under the same quality control as those of actual plant components in order to obtain reliable data about their behaviour.

- CV : 1/3.7 model of a 800MWe class steel reactor containment vessel
- RV : 1/1.5 model of a 1100MWe class reactor vessel (frequency was adjusted to 1/0.72 of the full size vessel by compensation masses)
- CI : 1/1 model of a 1100MWe class core (partial core model)
- RCS : 1/2.5 model of one reactor coolant loop of a 1100MWe class PWR(frequency was adjusted to 1/0.7 of the full size loop by compensation masses)

Outline drawings of the test models are shown in Fig.1.1 ~Fig.1.4 and the law of similitude is shown in Table 1.

3. TEST CONDITION

3.1 Input seismic waves

Of the various kinds of waves, those which gave the severest condition for each component were selected as the input waves for this test. The basic design earthquake ground motions S_1 and S_2, which have been improved and standardized by MITI for high seismic zones, were used as inputs to the reactor building analysis model of a standard PWR plant to obtain the floor response waves at the component support level. The selected response waves were then converted by the law of similitude to give the input waves for the test model. Table 2 shows the conditions of the input waves. As an example of input wave,Fig.2 shows the acceleration time history and the response spectrum of the S_2 (1) wave for CI test model. The models were simultaneously excited in the horizontal and vertical directions.

3.2 Environmental condition

Test conditions were as follows:

- CV : room temperature, atomospheric pressure,
- RV : room temperature. 15.4MPa, no flow,
- CI : room temperature, atomospheric pressure, no flow,
- RCS : room temperature, 15.4MPa, no flow.

4. TEST RESULTS

4.1 Reactor containment vessel

The distribution of the maximum response accelerations and stresses in the test model when excited by a S_2 wave together with a time history wave form for the acceleration of the top of the containment vessel are shown in Fig. 3.1 and Fig.3.2.

The results show that the responses due to oval vibration largely exceed those for beam type vibration because of the strong combination of the containment vessel and the polar crane vibrations. Consequently, it was found that the circumferential stresses exceeded the axial stresses. However, they were below the allowable level.

Leak rates measured before and after the containment vessel was excited by the seismic response acceleration waves S_1 and S_2 showed no significant difference. Therefore, the function of the reactor containment vessel was unaffected by the seismic motion.

The test model was simultaneous excited in the horizontal and vertical directions with a vibration wave equal to 1.5 times S_2 (horizontal: 3279 Gal, vertical: 1394 Gal). Adequate strength at 1.5 times excitation was confirmed since no abnomal phenomenon occurred.

As a result of comparing test and analysis data, it was recommended that the polar crane be modeled as a concentrated mass in the case of excitation pararell to the crane girder and that it be modeled as a distributed mass in the case of excitation perpendicular to the crane girder when the combined vibration analysis of the containment vessel and the polar crane is done.

4.2 Reactor Vessel

Maximum response accelerations, loads and stresses due to the S_1 and S_2 excitations are shown in Table 3 and the maximum response acceleration distribution for the S_2(1) excitation is shown in Fig. 4. Maximum stresses of the RV nozzle and support structure, which are the support points, were 24.5MPa(2.5kg/mm²) and 12.7MPa(1.3kg/mm²), respectively.

After the strength proving test, tests were carried out using the S_2 (2) seismic response wave with increased acceleration levels to check the seismic design margin. In addition to excitation with the normal support condition (8-nozzle support), a test with 4-nozzle support was carried out to increase the load per nozzle by reducing the number of supports. Fig.5 shows the response at the nozzle at increasing vibration levels. During the test, the maximum load on the nozzle of the test model reached approximately six times the S_2 load and almost twice the design value, but no abnormality was found in the post-test inspection. So, the RV was confirmed to have adequate margins for seismic strength.

4.3 Reactor Core Internals

The results of stress measurements on the test components are shown in Table 4 and the maximum response acceleration distribution under the 1.5 S_2(1) excitiation is shown in Fig. 6. It was observed that some local deformations of the fuel assembly grids occurred at high levels of excitaion.

Fig.7 shows the results of the control rod insertion time measurements during the excessive vibration test and for various seismic wave excitations. During all the tests, the control rods were inserted satisfactorily, and the increased drop time due to the earthquake was not significant, although the drop time became slightly longer as the excitation level increased.

When fuel assemblies vibrate, they collide either with one another or with the baffle plate. Fig.8 shows the relation between the maximum grid impact force and input acceleration for various configurations of fuel assemblies. Some discrepancy was recognized between the prediction analysis and the measured value. So, the analysis code was improved by taking account of a dependence of resonant frequency and damping on the vibration amplitude of the fuel assembly, and also by considering higher mode vibrations. Examples of comparisons between measurement results and the simulation analysis are shown in Fig.8 and Fig.9. Fairly good agreement is obtained between the test results and the analysis data.

4.4 Primary Coolant Loop System

The maximum response acceleration distribution for the S_2 response wave excitation is shown in Fig.10. Analysis results are also shown in the same figure.

Table 5 shows measured values and analysis results for piping stresses and support loads.

The integrity of the test model was confirmed by increased the excitation to twice the original $S_2(2)$ wave horizontally and 1.5 times vertically which corresponded to the excitation limit of the vibration table. Fig.11 shows stress values of the reactor coolant pipe.

Time intervals of the S_2 seismic wave were adjusted so that the predominant period of the seismic wave coincided with the natural period of the test model; thus making a resonant wave. The strength margin was confirmed by exciting the model with the resonant wave so that the snubber load reached twice the design value. Fig.12 shows the snubber reaction forces at the top of the steam generator for various resonant S_2 wave inputs. In this case, stress in the snubber pistons reached 562MPa (57.3kg/mm²) for the steam generator upper shell snubbers, exceeding the design allowable stress of 488MPa(49.8kg/mm²).

No abnormality was observed in the post test inspection. For the snubbers in particular, visual inspection, pressure proof test/inspection, performance confirmation test/inspection, and disassembly/inspection, were carried out to confirm their integrity, and no abnormality such as damage, deformation, looseness or oil leak was observed. The snubber performance was maintained both for strength and sealing ability.

5. CONCLUSION

Seismic proving test of four PWR test models were carried out using the large-scale high performance shaking table. The results of these proving tests are summarized as follows.

(1) Reactor containment, reactor vessel, reactor core internals (fuel assemblies) and primary coolant loop system, which are key components from the point of view of seismic reliability, were confirmed to have adequate strength and to maintain their function with sufficient margin during the severest seismic event which is postulated in the actual plant design.

(2) On the basis of the comparison of the test results and the simulation analysis, the appropriateness of the current seismic design analysis method was confirmed.

ACKNOWLEDGEMENT

This test project was conducted under the sponsorship of the Ministry of International Trade and Industry. The authors express their sincere gratitude to the members of the committee for the contribution to the successful completion of the PWR seismic proving test.

REFERENCES

Ohmori, T. et al. 1985. Proving test on the seismic reliability for nuclear power plant, PWR reactor containment vessel. NUPEC Report.

Ohmori, T. et al. 1987. Proving test on the seismic reliability for nuclear power plant, PWR reactor internals. NUPEC Report.

Kawakami, S. et al. 1991. Proving tests on the seismic reliability for nuclear power plant, PWR primary coolant loop system. NUPEC Report.

Kawakami, S. et al. 1992. Proving tests on the seismic reliability for nuclear power plant, PWR reactor vessel. NUPEC Report.

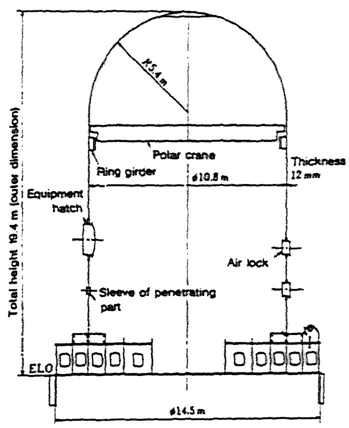

Fig.1.1 Test model for PWR reactor containment vessel

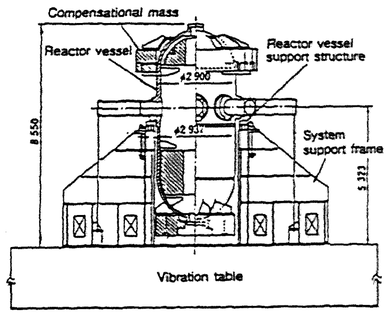

Fig.1.2 Test model for PWR reactor vessel

Table 1 Law of similitude applied to PWR test models

Physical quantity	Notation	Law of similitude	Ratio CV	RV	CI	RCS
Length	L	$L_m/L_p=1/N$	1/3.7	1/1.5	1	1/2.5
Cross section	A	$A_m/A_p=1/N^2$	1/13.69	1/2.25	1	1/6.25
Young's modulus	E	$E_m/E_p=1$	1	1	1	1
Strain	ε	$\varepsilon_m/\varepsilon_p=1$	1	1	1	1
Stress	σ	$\sigma_m/\sigma_p=1$	1	1	1	1
Displacement	x	$x_m/x_p=1/N$	1/3.7	1/1.5	1	1/2.5
Force	P	$P_m/P_p=1/N^2$	1/13.69	1/2.25	1	1/6.25
Frequency	f	$f_m/f_p=1/X$	3.7	1/0.72	1	1/0.7
Acceleration	α	$\alpha_m/\alpha_p=(1/X^2)/N$	3.7	1/0.778	1	1/1.225
Time	t	$t_m/t_p=X$	1/3.7	0.72	1	0.7
Weight	w	$w_m/w_p=X^2/N$	1/50.653	1/2.894	1	1/5.102
Spring constant	k	$k_m/k_p=1/N$	1/3.7	1/1.5	1	1/2.5

Note: Suffix m: model, p: actual plant N: scaling factor X: frequency ratio

Table 2 Input waves for proving tests

	CV M, Δ	CV α_{max} (Gal)	RV M, Δ	RV α_{max} (Gal)	CI M, Δ	CI α_{max} (Gal)	RCS M, Δ	RCS α_{max} (Gal)
S_1 [1]	M≒7.0 Δ≒20km	H : 1425 V : 590	M=7.0 Δ=20km	H : 480 V : 155	M=8.4 Δ=90km	H : 408 V : 151	M=7.0 Δ=20km	H : 433 V : 98
S_2(1) [2]	M≒8.5 Δ≒68km	H : 2186 V : 929	M=6.5 Δ=7.2km	H : 969 V : 217	M=8.5 Δ=68km	H : 729 V : 252	M=6.5 Δ=7.2km	H : 904 V : 138
S_2(2) [2]			—	H : 918 V : 526	—	H : 714 V : 375	—	H : 1190 V : 334

1) S_1 : Response wave of maximum design earthquake — improved and standardized plant for high seismic zones

2) S_2 : Response wave of extreme design earthquake
(1) Improved and standardized plant for high seismic zones
(2) Actual 4-loop PWR plant design wave (high seismic zone, seismic wave enveloping distant and near earthquakes)

Table 3 Maximum response results for the RV test

Measuring Item / Measuring Point	S_1 vibration test	S_2 (1) vibration test	S_2 (2) vibration test
ACCELERATION			
RV top	467 gal	992 gal	960 gal
RV nozzle	447 gal	930 gal	889 gal
RV bottom	620 gal	1242 gal	1572 gal
NOZZLE LOAD			
horizontal	39 ton	75 ton	75 ton
vertical	25 ton	53 ton	68 ton
STRESS			
RV nozzle	1.0 kgf/mm²	2.0 kgf/mm²	2.5 kgf/mm²
RV support	0.5 kgf/mm²	1.1 kgf/mm²	1.3 kgf/mm²

Table 4 Results of stress measurements during CI tests

[Kgf/mm²]

Component	S_1	S_2 (1)	S_2 (2)	Reference yield strength (20℃)
Fuel assembly				
Fuel cladding	2.8	3.2	2.9	62.3
Control rod guide thimble	7.4	8.4	7.9	24.6
Control rod drive mechanism (CRDM)	1.8	2.7	3.3	21.0
Core internals				
RCC guide tube	1.3	1.8	0.7	21.0
Core barrel	0.4	0.9	0.9	21.0

Table 5 Support loads and pipe stresses for the RCS tests (measurement/analysis) (Unit: load [ton], stress [kgf/mm²])

Components \ Load/Stress \ Input earthquake	S_1 wave Test result	S_1 wave Analysis (h=3%)	S_2 (1) wave Test result	S_2 (1) wave Analysis (h=3%)	S_2 (2) wave Test result	S_2 (2) wave Analysis (h=3%)
<Steam generator load>						
Upper shell support structure	24.9	22.0	51.8	56.6	61.0	62.2
Intermediate shell support structure	12.4	30.8	43.8	77.6	49.5	94.4
Lower support structure	3.4	1.4	6.2	3.4	11.0	5.0
Support column	19.4	17.3	32.4	36.1	68.9	58.2
<Reactor coolant pump load>						
Upper support structure	2.7	2.2	6.3	4.9	8.9	7.2
Lower support structure	3.2	1.8	5.9	4.2	7.5	7.0
Support column	5.0	4.9	10.4	11.1	17.8	16.5
<Reactor coolant pipe stress>						
Hot leg	*0.90*	*1.25*	*2.40*	*3.11*	*3.52*	*3.92*
Crossover leg	0.54	1.04	1.20	2.34	2.20	2.90
Cold leg	0.64	1.15	1.48	2.48	2.16	3.74

(Notes) • Piping stress (σ) is obtained by a calculation of max.strain (ε) at measuring point multiplied by Young's modulus (E) .($\sigma=\varepsilon E$)

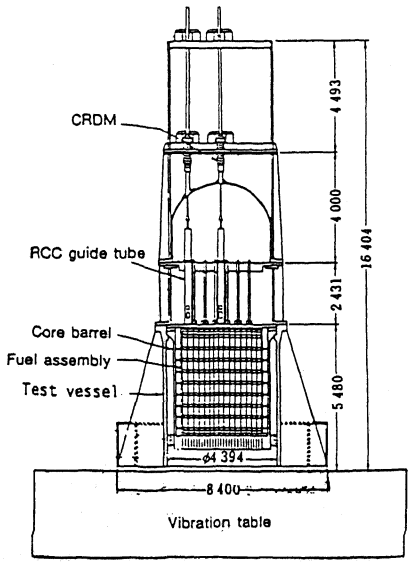

Fig.1.3 Test model for PWR reactor core internals

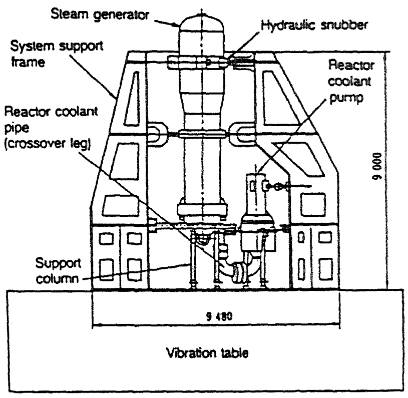

Fig.1.4 Test model for PWR primary coolant loop system

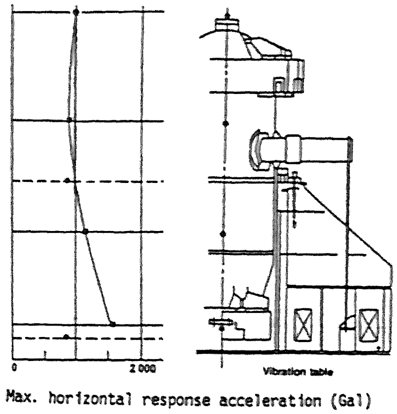

Fig.4 Distribution of maximum response accelerations at S_2 (1) excitation (RV test)

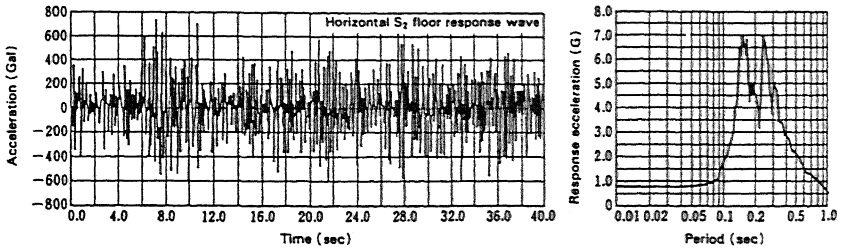

Response spectrum of horizontal S_2 acceleration (damping : 1%)

Fig.2 An example of input wave (CI test)

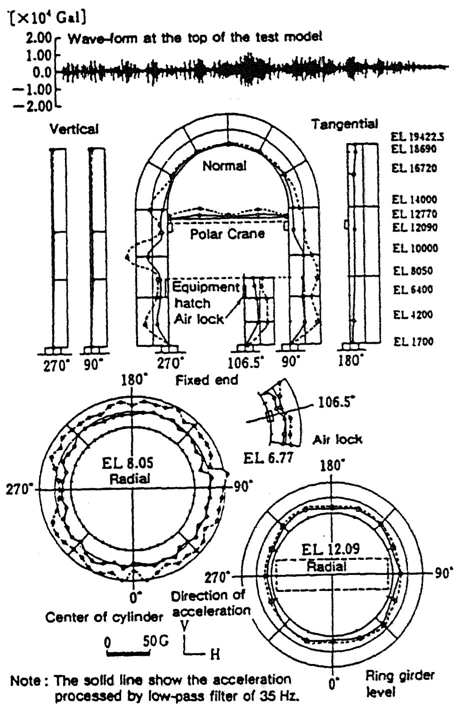

Fig.3.1 Distribution of maximum response accelerations at S_2 excitation (CV test)

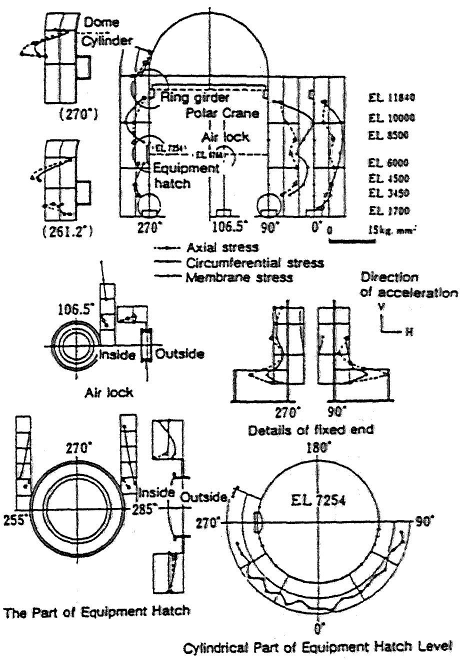

Fig.3.2 Distribution of maximum response stresses at S_2 excitation (CV test)

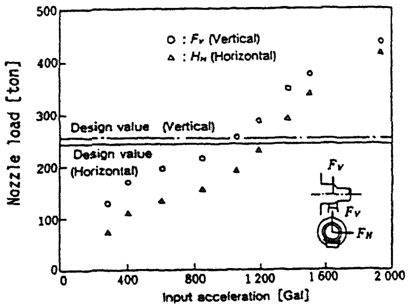

Fig.5 Reactor vessel responses to input acceleration

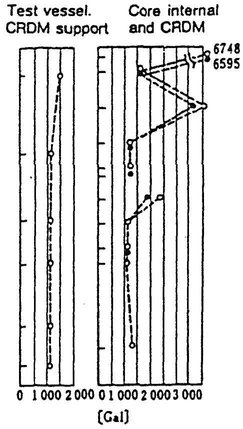

Fig.6 Maximum response accelerations at 1.5 S_2 (1) excitation (CI test)

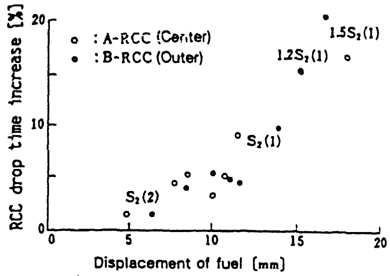

Fig.7 Relation between RCC drop time increase and response of test model

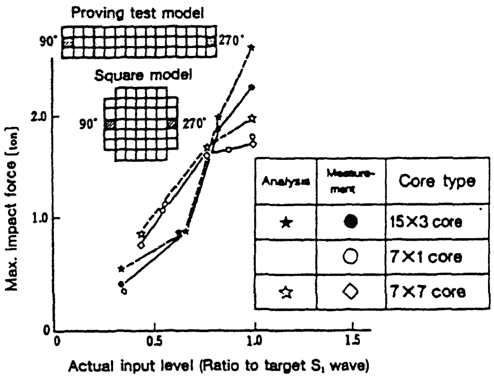

Fig.8 Relation between impact force on fuel grids and input level for the various test configurations

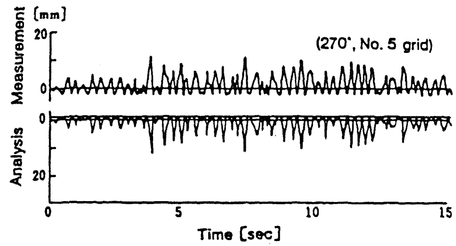

Fig.9 Comparison of measurement and simulation analysis by improved code (15 ×3 core, S_1 wave, fuel assembly displacement)

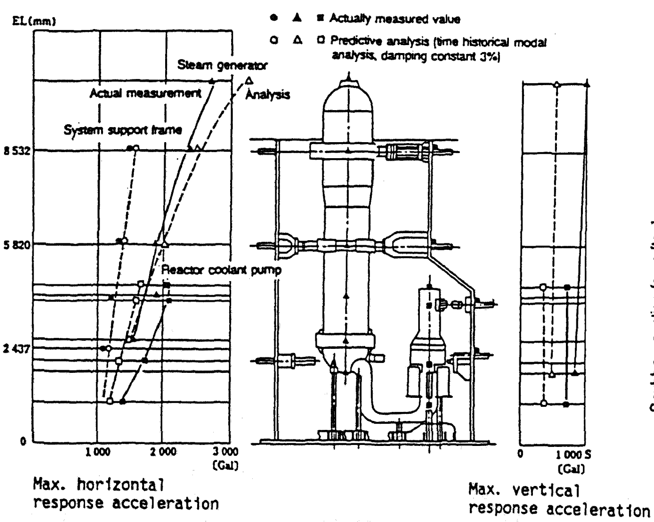

Fig.10 Distribution of maximum response accelerations at S_2(2) excitation (RCS test)

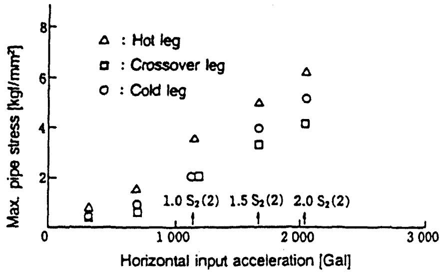

Fig.11 Stress in reactor coolant pipe (increased S_2 wave)

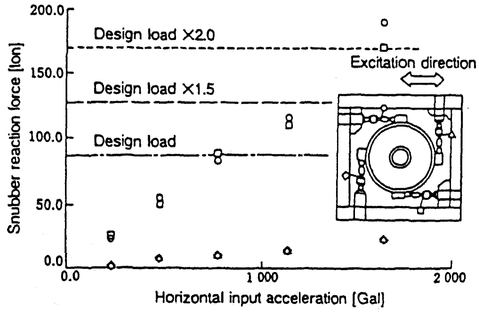

Fig.12 Response loads of steam generator upper shell snubbers (resonant S_2 wave)